Longitudinal Analysis of Pre-term Neonatal Brain Ventricle in Ultrasound Images Based on Convex Optimization

Wu Qiu[1,⋆], Jing Yuan[1,⋆], Jessica Kishimoto[1], Yimin Chen[2], Martin Rajchl[3], Eranga Ukwatta[4], Sandrine de Ribaupierre[5], and Aaron Fenster[1]

[1] Robarts Research Institute, University of Western Ontario, London, ON, CA
[2] Department of Electronic Engineering, City University of Hong Kong, CN
[3] Department of Computing, Imperial College London, London, UK
[4] Sunnybrook Health Sciences Centre, Toronto, CA; Department of Biomedical Engineering, Johns Hopkins University, MD, USA
[5] Neurosurgery, Department of Clinical Neurological Sciences, University of Western Ontario, London, ON, CA

Abstract. Intraventricular hemorrhage (IVH) is a major cause of brain injury in preterm neonates and leads to dilatation of the ventricles. Measuring ventricular volume quantitatively is an important step in monitoring patients and evaluating treatment options. 3D ultrasound (US) has been developed to monitor ventricle volume as a biomarker for ventricular dilatation and deformation. Ventricle volume as a global indicator, however, does not allow for the precise analysis of local ventricular changes. In this work, we propose a 3D+t spatial-temporal nonlinear registration approach, which is used to analyze the detailed local changes of the ventricles of preterm IVH neonates from 3D US images. In particular, a novel sequential convex/dual optimization is introduced to extract the optimal 3D+t spatial-temporal deformable registration. The experiments with five patients with 4 time-point images for each patient showed that the proposed registration approach accurately and efficiently recovered the longitudinal deformation of the ventricles from 3D US images. To the best of our knowledge, this paper reports the first study on the longitudinal analysis of the ventriclar system of pre-term newborn brains from 3D US images.

Keywords: 3D ultrasound, pre-term neonatal ventricles, spatial-temporal registration, convex optimization.

1 Introduction

Ventriculomegaly (VM) is often seen in pre-term neonates born at < 32 weeks gestation or with very low birth weight (< 1500 g). Intraventricular hemorrhage (IVH) is one of the primary non-congenital causes of VM, which is caused by bleeding in the brain that occurs in 15-30% of very low birth weight pre-term neonates and is predictive of an adverse neurological outcome [9]. Preterm infants

⋆ Contributed equally.

N. Navab et al. (Eds.): MICCAI 2015, Part III, LNCS 9351, pp. 476–483, 2015.
DOI: 10.1007/978-3-319-24574-4_57

with IVH are at risk of white matter injury, and the development of post hemorrhagic ventricular dilatation (PHVD) increases the risk of an adverse neurodevelopmental outcome. It is difficult to follow the dynamic of ventricle dilatation with current techniques (2D ultrasound (US) and MR imaging) determine the level by which ventricle dilatation is progressing. While clinicians have a good sense of what VM looks like compared to normal ventricles, there is little information available on how the cerebral ventricles change locally and temporally in pre-term IVH neonates. Additionally, the PHVD patients require interventional therapies, and about 20-40% of these patients will consequently develop hydrocephalus, necessitating surgery. Currently, there is no means of accurately predicting PHVD or determining if and when ventricular dilation requires treatment [14]. 3D US has proven to be a useful tool to measure the ventricle volume size, which can be used as a global indicator of ventricle changes [8,10]. However, differential enlargement of specific parts of the ventricles occurs over time, which cannot be identified by volume measurement alone. Thus, the longitudinal analysis of ventricle changes could provide rich information explaining some specific neurological and neuropsychological deficits, and can greatly improve the diagnosis, prognosis, and treatment of VM [3]. Longitudinal analysis of brains has been extensively studied using MR images, mostly focusing on adult populations, leading to several successful methods and software packages, such as SPM [1], FreeSurfer [7], and aBEAT [6]. However repeated MRI are not feasible in the context of preterm infants, as they are too weak to leave the unit for the first few weeks of their life. There are a few studies on the development of early brains [4,5]. However, methods employed for the longitudinal analysis of MR images are not suited for the unique challenges posed by US imaging, such as US image speckle, low tissue contrast, fewer image details of structures, and dramatic inter-subject shape deformation [8,10]. In addition, 3D neonatal US images can only provide the partial view of the neonatal brain, rather than the whole brain as in 3D MR images.

Contributions: A novel 3D+t deformable image registration technique is developed for the longitudinal analysis of 3D neonatal ventricle US images, which makes use of a sequential convex optimization technique to address the resulting nonlinear and non-smooth image fidelity function. Each convex optimization sub-problem is solved under a dual optimization perspective. The developed approach allows for the registration of all the follow-up 3D ventricle US images onto the baseline image in the same spatial coordinates. To the best of our knowledge, this paper reports the first study on the longitudinal analysis of lateral ventricles of pre-mature newborn brains from the temporal sequence of 3D US images.

2 Method

Optimization Model: Given a sequence of 3D US images $I_1(x) \ldots I_{n+1}(x)$, we aim at computing the temporal sequence of 3D deformation fields $u_k(x)$, $k = 1 \ldots n$, within each two adjacent images $I_k(x)$ and $I_{k+1}(x)$, while imposing both spatial and temporal smoothness of the 3D+t spatial-temporal deformation fields $u_k(x) = (u_k^1(x), u_k^2(x), u_k^3(x))^{\mathrm{T}}$, $k = 1 \ldots n$.

In this work, we apply the sum of absolute intensity differences (SAD) to evaluate the dissimilarities between each two adjacent images $I_k(x+u_k(x))$ and $I_{k+1}(x)$, $k=1\dots n$, over the deformation field $u_k(x)$. Hence, we have

$$P(I_{1\dots n+1};u) := \sum_{k=1}^{n} \int_{\Omega} |I_k(x+u_k(x)) - I_{k+1}(x)| \, dx \tag{1}$$

to measure the 3D+t intensity-based dissimilarities within the input 3D image sequence I_k, over the sequence of 3D deformation fields $u_k(x)$, $k=1\dots n$.

For each 3D deformation field $u_k(x)$, $k=1\dots n$, we prefer a smooth deformation field, hence penalize its spatial non-smoothness; in this work, we minimize the convex quadratic function of the spatial non-smoothness of deformations, *i.e.*,

$$R(u) := \alpha \sum_{k=1}^{n} \int_{\Omega} \left(\left|\nabla u_k^1\right|^2 + \left|\nabla u_k^2\right|^2 + \left|\nabla u_k^3\right|^2 \right) dx \,, \tag{2}$$

where $\alpha > 0$ is the positive spatial regularization parameter. Actually, spatial regularization function significantly restricts the solution space of deformation fields and sets up the well-posedness of the deformable registration problem. In addition, we also employ a temporal smoothness prior which encourages the similarities between each two adjacent deformation fields $u_k(x)$ and $u_{k+1}(x)$, $k=1\dots n-1$, and penalizes their total absolute differences, *i.e.*,

$$T(u) := \gamma \sum_{k=1}^{n-1} \int_{\Omega} \left(\left|u_k^1 - u_{k+1}^1\right| + \left|u_k^2 - u_{k+1}^2\right| + \left|u_k^3 - u_{k+1}^3\right| \right) dx \,, \tag{3}$$

where $\gamma > 0$ is the temporal regularization parameter. Such absolute function-based proposed temporal regularization function (3) can eliminate undesired sudden changes within each two neighbouring deformation fields, which is mainly due to the poor image quality of US including US speckle and shadows, low tissue contrast, fewer image details of structures, and improve robustness of the introduced 3D+t non-rigid registration method.

Considering (1), (2) and (3), we formulate the studied 3D+t deformable registration of the input 3D US image sequence as the following optimization problem:

$$\min_{u_{1\dots n}(x)} \; P(I_{1\dots n+1};u) \; + \; R(u) \; + \; T(u) \,, \tag{4}$$

where the spatial and temporal regularization functions $R(u)$ and $T(u)$ allow the well-posed optimization formulation (4).

Sequential Convex and Dual Optimization: The image fidelity term $P(I_{1\dots n+1};u)$ of (4) is highly nonlinear, which is challenging to be minimized directly. In this regard, we use an incremental Gauss-Newton optimization scheme [2], which results in a series of linearization of the nonlinear function $P(I_{1\dots n+1};u)$ over the incremental warping steps, hence a sequence of convex optimization problems, where each convex optimization problem properly computes an optimal update $h(x)$ to the current deformation approximation $u(x)$, till convergence, *i.e.*, the updated deformation $t(x)$ is sufficiently small.

Given the current estimated deformation $u(x)$, the linearization of $P(I_{1\dots n+1}; u+h)$ over its incremental update $h(x)$ gives rise to the following approximation:

$$P(I_{1\dots n+1}; u+h) \simeq \left(\tilde{P}(h) := \sum_{k=1}^{n} \int_{\Omega} \left| \nabla \tilde{I}_k \cdot h_k + \tilde{G}_k \right| dx\right), \tag{5}$$

where $\tilde{I}_k := I_k(x + u_k(x))$, $i = 1 \dots n$, denotes the deformed image $I_k(x)$ over the current deformation field $u_k(x)$, and $\tilde{G}_k := I_k(x + u_k(x)) - I_{k+1}(x)$.

Therefore, we can compute each deformation update $h(x)$ by solving the following optimization problem

$$\min_{h_{1\dots n}(x)} \sum_{k=1}^{n} \int_{\Omega} \left| \nabla \tilde{I}_k \cdot h_k + \tilde{G}_k \right| dx \; + \; R(u+h) \; + \; T(u+h)\, dx\,, \tag{6}$$

which is convex, due to the convexity of the absolute function and the spatial-temporal regularization functions $R(\cdot)$ and $T(\cdot)$, and can be optimized globally. Note that a small number n of time point images leads to approximation errors in practice, and a large number n results in a more smooth temporal deformation field.

Dual Optimization Formulation. In this work, we solve the convex minimization problem (6) under a dual-optimization perspective, which not only avoids directly tackling the non-smooth functions of (6) but also derives a new duality-based algorithm. Moreover, the proposed dual optimization-based approach can be easily extended to minimize the energy function (6) with any other spatial and temporal regularizars, for example the non-smooth total-variation based regularization function $\sum_{i=1}^{3} \int_{\Omega} |\nabla(u)|\, dx$.

Through variational analysis, we can derive a mathematically equivalent *dual model* to the convex minimization problem (6):

Proposition 1. *The convex minimization problem* (6) *can be equally reformulated by its* dual model*:*

$$\begin{aligned} \max_{w,q,r} \sum_{k=1}^{n} \int_{\Omega} \left(w_k \tilde{G}_k \; + \; \sum_{i=1}^{n} u_k^i \operatorname{div} q_k^i\right) dx \; - \; \frac{1}{2\alpha} \sum_{k=1}^{n} \sum_{i=1}^{3} \int_{\Omega} \left(q_k^i\right)^2 dx \\ + \sum_{k=1}^{n-1} \sum_{i=1}^{3} \int_{\Omega} \left(r_k^i (u_k^i - u_{k+1}^i)\right) dx \end{aligned} \tag{7}$$

subject to

$$F_1^i(x) := (w_1 \cdot \partial_i \tilde{I}_1 + \operatorname{div} q_1^i + r_1^i)(x) \; = \; 0\,, \tag{8}$$

$$F_k^i(x) := (w_k \cdot \partial_i \tilde{I}_k + \operatorname{div} q_k^i + (r_k^i - r_{k-1}^i))(x) \; = \; 0\,, \quad k = 2 \dots n-1\,, \tag{9}$$

$$F_n^i(x) := (w_n \cdot \partial_i \tilde{I}_n + \operatorname{div} q_n^i - r_{n-1}^i)(x) \; = \; 0\,, \tag{10}$$

where $i = 1 \dots 3$*, and*

$$|w_k(x)| \; \leq \; 1\,, \;\; \left|r_k^1(x)\right| \; \leq \; \gamma\,, \;\; \left|r_k^2(x)\right| \; \leq \; \gamma\,, \;\; \left|r_k^3(x)\right| \; \leq \; \gamma\,;\; k = 1 \dots n\,.$$

The proof follows the facts that $\gamma|x| = \max_{|w|\leq\gamma} wx$, and the convex optimization problem (6) can be equally rewritten by the minimax of its associated primal-dual Lagrangian function, *i.e.*,

$$\min_{h}\max_{w,q,r} L(h,w,q,r) := \sum_{k=1}^{n}\int_{\Omega}\left(w_k\tilde{G}_k + \sum_{i=1}^{n} u_k^i \operatorname{div} q_k^i\right)dx - \frac{1}{2\alpha}\sum_{k=1}^{n}\sum_{i=1}^{3}\int_{\Omega}\left(q_k^i\right)^2 dx + \sum_{k=1}^{n-1}\sum_{i=1}^{3}\int_{\Omega}\left(r_k^i(u_k^i - u_{k+1}^i)\right)dx + \sum_{k=1}^{n}\sum_{i=1}^{3}\left\langle h_k^i, F_k^i\right\rangle, \quad (11)$$

subject to $|w(x)| \leq 1$ and $\left|r_k^i(x)\right| \leq \gamma$, $i = 1,2,3$; where the functions $F_k^i(x)$, $k = 1\ldots n$ and $i = 1,2,3$, are defined in (8). We refer to [15,11,12] for the detailed primal-dual analysis. Given Prop. 1 and the Lagrangian function (11), each component of the incremental deformation $h_k(x)$ just works as the multiplier function to the respective linear equalities (8) under the primal-dual perspective. In addition, the associated primal-dual energy function of (11) is just the Lagrangian function to the *dual formulation* (7), which can be solved by an efficient duality-based Lagrangian augmented algorithm [15,11,12].

3 Experiments and Results

Image Acquistion: A motorized 3D US system developed for cranial US scanning of pre-term neonates was used for image acquisition in the neonatal intensive care unit (NICU) [8]. The 3D image sizes ranged from $300 \times 300 \times 300$ to $450 \times 450 \times 450$ voxels with a voxel spacing of $0.22 \times 0.22 \times 0.22$ mm^3. Five patients were enrolled in this study. Once enrolled, patients underwent serial US exams 1-2 times per week until the discharge from NICU, or transfer to a secondary care center. Four time-point 3D images were acquired per patient. Each

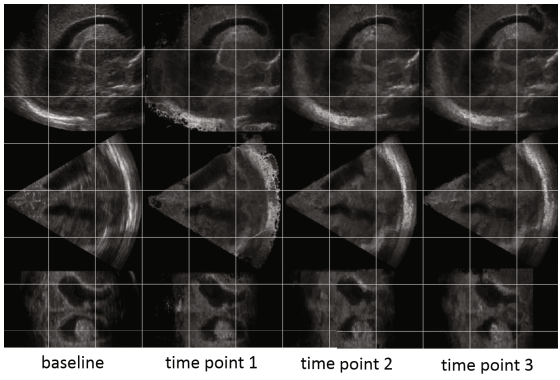

Fig. 1. Registration results of an IVH neonatal ventricles in 3D US image. 1 - 4 columns: baseline, registered images at time points 1-3. The first - third row: sagittal, coronal, and transvers view.

image was manually segmented on parallel sagittal slices by a trained observer and verified by an experienced clinician. Manual segmentations were used to evaluate the 3D+t registration results.

Evaluation Metrics: Our registration method was evaluated by comparing the registered follow-up image with the corresponding baseline image in terms of the overlap of two ventricle surfaces extracted from the two images using *volume-based metrics*: Dice similarity coefficient (DSC); and *distance-based metrics*: the mean absolute surface distance (MAD) and maximum absolute surface distance (MAXD) [11,12].

Results: Figure 1 shows an example of registered follow-up and baseline images from transverse, coronal and sagittal views. Table 1 summarizes the quantitative registration results for the initial rigid alignment, pair-wise deformable registration without the spatial-temporal constraint [13], and the proposed 3D+t non-linear registration, which shows that the proposed 3D+t deformable registration improved the target ventricle overlap in terms of DSC, MAD, and MAXD, compared to the results after rigid registration and pair-wise deformable registration without the spatial-temporal constraint. The ventricles at each time point were additionally compared to the previous time point using the generated 3D+t deformation results. The local 3D volume changes can be well represented by the divergence of deformations, *i.e.*, $\operatorname{div} u(x) := (\partial_1 u_1 + \partial_2 u_2 + \partial_3 u_3)(x)\,, \quad \forall x \in \mathcal{R}_{ventricle}$. The local volume changes within the ventricle regions over the computed deformation field $u_k(x)$ are shown in Fig. 2.

The proposed 3D+t non-rigid registration algorithm was implemented in Matlab (Natick, MA), and the experiments were conducted on a Windows desktop with an Intel i7-2600 CPU (3.4 GHz). The registration time was calculated as the mean run time of five registrations. The mean registration time of our method was 8.1 ± 1.2 minutes per patient dataset.

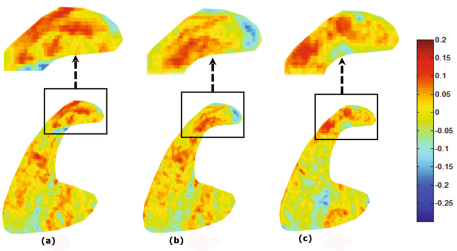

Fig. 2. Local volume changes represented by the divergence of the deformation field, *i.e.*, $\operatorname{div} u(x)$, at each time point. (a)-(c): the first-third time points. The local volume expansion is colored in red, while the local volume shrinkage is colored in blue. Magnifications of all regions of interest are depicted in the top row.

Table 1. Registration results of 5 patient images (4 time points each patient) in terms of DSC, MAD, and MAXD (p1-p5: patient ID), represented as the mean ± standard deviation.

	DSC (%)	MAD (mm)	MAXD (mm)
Rigid	66.4 ± 4.3	1.2 ± 1.3	7.0 ± 4.4
Pair-wise nonlinear registration	78.5 ± 3.3	0.7 ± 0.8	3.8 ± 3.0
3D+t nonlinear registration	$\mathbf{80.1 \pm 2.4}$	$\mathbf{0.5 \pm 0.6}$	$\mathbf{3.1 \pm 2.2}$

4 Discussion and Conclusion

Longitudinal analysis of 3D neonatal brain US images can reveal structural and anatomical changes of neonatal brains during aging or in patients with IVH disease. The analysis has the potential to be used to monitor patients and evaluate treatment options with quantitative measurements of ventricular dilatation or shrinkage in pre-term IVH neonates over time. The unique challenges provided by 3D US images of neonatal brains make most registration-based analysis methods used in MR images not useful. To cater for this clinical need, a deformable 3D+t registration approach is proposed to accurately and efficiently analyze the longitudinal pre-term neonatal brain from 3D US images. Specifically, the proposed 3D+t registration approach makes use of convex and dual optimization technique to efficiently extract the optimal 3D+t spatial-temporal deformation field and enjoys both efficiency and simplicity in numerics. In addition, the proposed dual optimization-based algorithm can be parallelized on GPUs to accelerate the computation.

The experimental results show that the proposed 3D+t registration approach can capture the longitudinal deformation of neonatal ventricles in 3D US images accurately and efficiently, suggesting that it could help physicians to locally quantify the neonatal ventricle changes over time. The proposed method was preliminarily evaluated on a small database. Additional validation on a large number of images would be required. Future work will involve mapping different subject images onto a healthy template image for classification of disease grade and progression. Moreover, based on the developed registration technique, an IVH-grade- and age-specific 3D US neonatal ventricle atlas may clinically useful for the diagnosis and treatment of developing neonatal brains with VM.

Acknowledgments. The authors are grateful for the funding support from the Canadian Institutes of Health Research (CIHR) and Academic Medical Organization of Southwestern Ontario (AMOSO).

References

1. Ashburner, J., Friston, K.J.: Unified segmentation. NeuroImage 26(3), 839–851 (2005)
2. Baust, M., Zikic, D., Navab, N.: Diffusion-based regularisation strategies for variational level set segmentation. In: BMVC, pp. 1–11 (2010)
3. Breeze, A.C., Alexander, P., Murdoch, E.M., Missfelder-Lobos, H.H., Hackett, G.A., Lees, C.C.: Obstetric and neonatal outcomes in severe fetal ventriculomegaly. Prenatal Diagnosis 27(2), 124–129 (2007)
4. Chen, Y., An, H., Zhu, H., Jewells, V., Armao, D., Shen, D., Gilmore, J.H., Lin, W.: Longitudinal regression analysis of spatial–temporal growth patterns of geometrical diffusion measures in early postnatal brain development with diffusion tensor imaging. NeuroImage 58(4), 993–1005 (2011)
5. Dai, Y., Shi, F., Wang, L., Wu, G., Shen, D.: ibeat: a toolbox for infant brain magnetic resonance image processing. Neuroinformatics 11(2), 211–225 (2013)
6. Dai, Y., Wang, Y., Wang, L., Wu, G., Shi, F., Shen, D., Initiative, A.D.N., et al.: abeat: A toolbox for consistent analysis of longitudinal adult brain mri. PloS One 8(4), e60344 (2013)
7. Fischl, B., Salat, D.H., Busa, E., Albert, M., Dieterich, M., Haselgrove, C., van der Kouwe, A., Killiany, R., Kennedy, D., Klaveness, S., et al.: Whole brain segmentation: automated labeling of neuroanatomical structures in the human brain. Neuron 33(3), 341–355 (2002)
8. Kishimoto, J., de Ribaupierre, S., Lee, D., Mehta, R., St Lawrence, K., Fenster, A.: 3D ultrasound system to investigate intraventricular hemorrhage in preterm neonates. Physics in Medicine and Biology 58(21), 7513 (2013)
9. Klebermass-Schrehof, K., Rona, Z., Waldhör, T., Czaba, C., Beke, A., Weninger, M., Olischar, M.: Can neurophysiological assessment improve timing of intervention in posthaemorrhagic ventricular dilatation? Archives of Disease in Childhood-Fetal and Neonatal Edition 98(4), F291–F297 (2013)
10. Qiu, W., Yuan, J., Kishimoto, J., McLeod, J., de Ribaupierre, S., Fenster, A.: User-guided segmentation of preterm neonate ventricular system from 3d ultrasound images using convex optimization. Ultrasound in Medicine & Biology 41(2), 542–556 (2015)
11. Qiu, W., Yuan, J., Ukwatta, E., Sun, Y., Rajchl, M., Fenster, A.: Dual optimization based prostate zonal segmentation in 3D MR images. Medical Image Analysis 18(4), 660–673 (2014)
12. Qiu, W., Yuan, J., Ukwatta, E., Sun, Y., Rajchl, M., Fenster, A.: Prostate segmentation: An efficient convex optimization approach with axial symmetry using 3D TRUS and MR images. IEEE Trans. Med. Imag. 33(4), 947–960 (2014)
13. Sun, Y., Yuan, J., Qiu, W., Rajchl, M., Romagnoli, C., Fenster, A.: Three-dimensional non-rigid mr-trus registration using dual optimization. IEEE Transactions on Medical Imaging 34(5), 1085–1094 (2015)
14. de Vries, L.S., Brouwer, A.J., Groenendaal, F.: Posthaemorrhagic ventricular dilatation: when should we intervene? Archives of Disease in Childhood-Fetal and Neonatal Edition 98(4), F284–F285 (2013)
15. Yuan, J., Bae, E., Tai, X.C.: A study on continuous max-flow and min-cut approaches. In: CVPR (2010)